Chinese Chemical Letters 34 (2023) 107644

Contents lists available at ScienceDirect

Chinese Chemical Letters

journal homepage: www.elsevier.com/locate/cclet

Bis-naphthalimide-based supramolecular self-assembly system for selective and colorimetric detection of oxalyl chloride and phosgene in solution and gas phase

Qingqing Wang[a], Huijuan Wu[a], Aiping Gao[a,*], Xuefei Ge[a], Xueping Chang[a,*], Xinhua Cao[a,b,*]

[a] College of Chemistry and Chemical Engineering&Green Catalysis and Synthesis Key Laboratory of Xinyang city, Xinyang Normal University, Xinyang 464000, China
[b] Department of Chemistry, Fudan University, Shanghai 200438, China

ARTICLE INFO

Article history:
Received 28 May 2022
Revised 19 June 2022
Accepted 23 June 2022
Available online 30 June 2022

Keywords:
Bis-naphthalimide
Self-assembly
Colorimetric detection
Multi-modes

ABSTRACT

Two bis-naphthalimide-based supramolecular gelators (**NN-3** and **NN-4**) with a little difference of position of amino groups were designed and synthesized for the detection of oxaloyl chloride and phosgene. Energy transfer could be occurred between two naphthalimide groups in molecules **NN-3** and **NN-4**. Yellow gels **NN-3** and **NN-4** were formed in some mixed solvents, and nanofibers with different size were obtained in these gels. The self-assembly processes of **NN-3** and **NN-4** in different solvents were investigated by UV-vis absorption, fluorescent spectra, SEM, FTIR, XRD and NMR. Gelators **NN-3** and **NN-4** could selectively detect oxaloyl chloride in solution and film states, but detect phosgene only in solution. **NN-3** exhibited the ratiometric detection ability towards oxaloyl chloride and phosgene with the low limit of detection (LOD) of 210 nmol/L and 90 nmol/L, respectively. **NN-4** as the corresponding control sample, it owned the higher LOD towards oxaloyl chloride and phosgene of 12.4 μmol/L and 64 μmol/L, respectively. Interestingly, films **NN-3** and **NN-4** could sensitively detect oxaloyl chloride gases with the low LOD of 2.0 ppm and 8.34 ppm, respectively. The detection mechanisms of **NN-3** and **NN-4** were well studied by ^{1}H NMR titration, HRMS and theoretical calculation.

Supramolecular gels as a kind of soft materials with three-dimensional network structure, which can be achieved by means of the noncovalent interactions such as hydrogen bonds, van der Waals forces, π-π stacking, dipole–dipole, ion−ion, charge-transfer, coordination interactions [1–10]. Supramolecular gels are reversible and sensitive to environmental changes including pH, temperature, ionic strength and other changes, and further brings significant alteration about their color, emission, gel state and self-assembly structures [11–16]. Supramolecular gels have been wide application in many fields such as pollutant removal, drug delivery, biosensors, catalysis, optoelectronics, enzyme immobilization, solar cells [17–28]. For example, the three-dimensional network in gel and exerogel sates facilitates the penetration of analytes, and large contact area will produce quick response [13].

Oxalyl chloride ($(COCl)_2$) and phosgene are highly toxic gases even at low concentration although they are widely used in industrial chemical processes [29–32]. Exposure to oxalyl chloride and phosgene will irritate individual respiratory system and skin, cause severe damage to the lungs of humans, and even induce death [33–35]. Therefore, it is of great significance to develop reliable, sensitive, prompt and convenient methods for the detection of $(COCl)_2$ and phosgene. Some methods and materials for the detection of $(COCl)_2$ and phosgene have been reported in recent years [36–40]. However, these methods have numerous disadvantages such as long analysis time, complicated sample processing, poor portability and high cost. In comparison, fluorescent detection methods have attracted more attention because of their great convenience, operational simplicity, low cost and high sensitivity [41,42]. Li and Wang have designed a dual sensor based on a fluorescent benzothiazole dye for $(COCl)_2$ and phosgene with the high sensitivity and selectivity [43]. $(COCl)_2$ and phosgene could be detected by some sensors reported by us [44,45], but they were not be obviously distinguished. Therefore, it is desiderated to develop new probes with highly sensitive and selective detection ability.

In this work, a novel fluorescent gelator (**NN-3**) containing two naphthalimide groups were designed and synthesized, which was

* Corresponding authors.
E-mail addresses: gaoapchem@163.com (A. Gao), xuepingchang@xynu.edu.cn (X. Chang), caoxh@xynu.edu.cn (X. Cao).

https://doi.org/10.1016/j.cclet.2022.06.067
1001-8417/

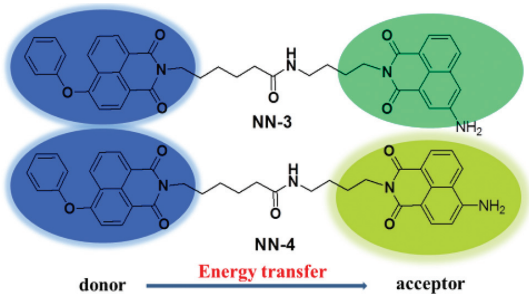

Scheme 1. Molecule structures of gelators **NN-3** and **NN-4**.

used as a self-assemble gel sensor for simultaneously selective detecting of oxalyl chloride and phosgene (Scheme 1). In molecule **NN-3**, the naphthalimide group with a terminal phenol at 4-position was as energy donor, and another naphthalimide group with an amidogen at 3-position was used as energy acceptor, and efficient energy transfer could be occurred between them. As a control molecule, a similar gelator molecule **NN-4** with an amidogen at 4-position of naphthalimide was produced, which only owned a little difference about the position of amidogen. Gelator **NN-3** exhibited better detection performance towards oxaloyl choride and phosgene than that of **NN-4**, and oxaloyl choride and phosgene could be differentiated *via* their different response time.

4-Amino-1,8-naphthalic anhydride, 3-amino-1,8-naphthalic anhydride, CH_3COCl, DCP, DECP, DMMP, $POCl_3$, tosyl chloride, oxalyl chloride, triphosgene and $SOCl_2$ were all purchased from shanghai Titan technology Co., Ltd. Other reagents were purchased from shanghai Darui finechemical Co., Ltd. All other reagents were analytical grade. To visually determine phosgene and its gas with this system, a predetermined amount of triphosgene/TEA (100 μmol/L) chloroform solution was placed in a centrifuge tube at room temperature for 5 min.

The gel abilities of **NN-3** and **NN-4** were investigated by the inverse flow method [44]. Films **NN-3** and **NN-4** were obtained by evaporation of solvent naturally. The detailed instrumentation information was listed in Supporting information.

Gelators **NN-3** and **NN-4** were synthesized according to our previous reported method (Scheme S1 in Supporting information) [46]. Solutions **NN-3** exhibited two absorption bands covering the range of 342-347 nm and 423-437 nm, which were assigned to π-π^* transitions of the naphthalimide group with a terminal phenol and naphthalimide group with an amino, respectively (Fig. S1a in Supporting information) [44]. Solutions **NN-4** also exhibited two absorption bands in the scopes of 360-367 nm and 405-436 nm in Fig. S1b (Supporting information). Solutions **NN-3** showed two emission peaks covering the range of 424-429 nm and 460-568 nm, which were assigned to the two naphthalimide groups (Fig. S1c in Supporting information). There was a specific different emission behavior for solution **NN-3** in ethyl acetate and toluene, which showed solvatochromism behavior. Solutions **NN-4** had a single emission peak located in the scope of 489-542 nm (Fig. S1d in Supporting information). Emission light of solutions **NN-3** and **NN-4** was from blue to green and yellow light with different intensity (Fig. S2 in Supporting information). Moreover, fluorescence quantum yield and lifetime of **NN-3** and **NN-4** were also investigated in different solvents (Table S2 in Supporting information). The absolute quantum yields of solutions **NN-3** and **NN-4** were in the range of 5.01%-32.87% and 12.13%-48.9% with the lifetime scope of 2.99-9.60 ns and 2.66-7.06 ns.

To verify the intramolecular energy transfer (ET), UV-vis absorption and fluorescence emission spectra of precursor compounds **1**-**3** in CH_2Cl_2 were done (Fig. 1). Compounds **1** and **2** had an absorption band at 361 nm and 405 nm, respectively. There

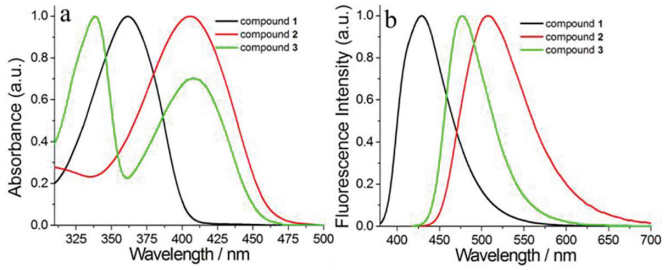

Fig. 1. UV-vis absorption spectra and fluorescence spectra of solutions **1**-**3** in CH_2Cl_2 with the concentration of 10^5 mol/L. The excitation wavelength for compounds **1**, **2** and **3** are 361, 405 and 408 nm, respectively.

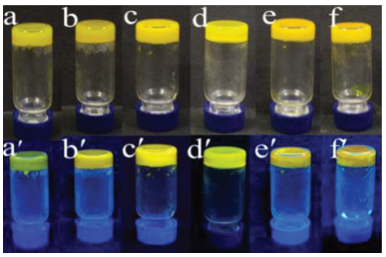

Fig. 2. Images of gels **NN-3** and **NN-4** in different solvent. (a, a′) **NN-3** for DMF/H_2O (v/v, 5/1); (b, b′) **NN-3** for DMSO/H_2O (v/v, 10/1); (c, c′) **NN-4** for DMF/H_2O (v/v, 5/1); (d, d′) **NN-4** for DMSO/H_2O (v/v, 10/1); (e, e′) **NN-4** for ethanol/H_2O (v/v, 10/1); (f, f′) **NN-4** for acetonitrile/H_2O (v/v, 10/1). The upper and lower were under daylight and 365 nm light, respectively.

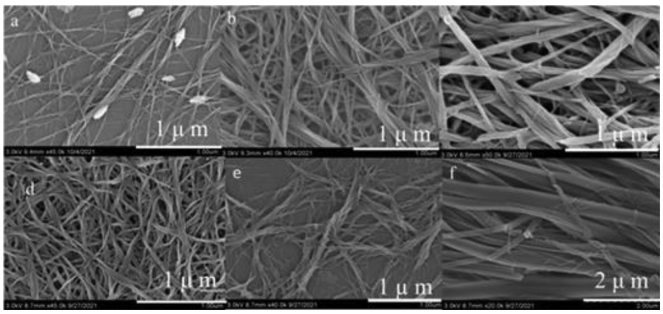

Fig. 3. SEM images of gels **NN-3** and **NN-4** in different solvents (a) **NN-3** in DMF/H_2O (v/v, 5/1); (b) **NN-3** in DMSO/H_2O (v/v, 10/1); (c) **NN-4** in DMF/H_2O (v/v, 5/1); (d) **NN-4** in DMSO/H_2O (v/v, 10/1); (e) **NN-4** in ethanol/H_2O (v/v, 10/1); (f) **NN-4** in acetonitrile/H_2O (v/v, 10/1). The scale bars of (a-f) are 1, 1, 1, 1, 1 and 2 μm.

were two absorption bands at 338 and 408 nm for solution **3**. Under the excitation of 361 nm, solution **1** emitted blue light at 428 nm, which was exactly overlapped by absorption band of compounds **2** and **3**. It was concluded that ET from the naphthalimide group with a terminal phenol to the naphthalimide group with an amino was happened in molecules **NN-3** and **NN-4** with different extents [47].

NN-3 could form gels only in DMSO/H_2O (v/v, 10/1) and DMF/H_2O (v/v, 5/1) with the critical gel concentration (CGC) of 5.68, 6.94 mg/mL (Table S2). Solutions and precipitates of **NN-3** were obtained in other solvents. **NN-4** could form gels in ethanol/H_2O (v/v, 10/1), acetonitrile/H_2O (v/v, 10/1), DMSO/H_2O (v/v, 10/1) and DMF/H_2O (v/v, 5/1) with the CGC of 9.09, 11.4, 5.68 and 6.94 mg/mL, respectively. Yellow gels **NN-3** and **NN-4** formed in these solvents emitted yellow-green light under 365 nm light (Fig. 2). **NN-3** self-assembled into nanofibers in its gels (Figs. 3a and b). The similar nanofiber structures were observed in gels **NN-4** from DMSO/H_2O (v/v, 10/1) and ethanol/H_2O (v/v, 10/1) (Figs. 3d and e). The bulky nanofibers were obtained in gels **NN-4**

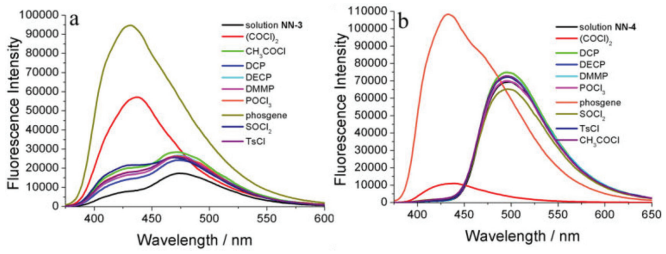

Fig. 4. Fluorescence emission spectra change of solutions (a) **NN-3** and (b) **NN-4** in CH_2Cl_2 upon the addition of different acyl chloride (1.0 equiv. and 50.0 equiv. for **NN-3** and **NN-4**). The concentrations of solutions **NN-3** and **NN-4** are 10 μmol/L.

from DMF/H_2O (v/v, 5/1) and acetonitrile/H_2O (v/v, 10/1) (Figs. 3c and f).

To explore the self-assembly modes of **NN-3** and **NN-4** in gel, UV-vis absorption spectra of **NN-3** and **NN-4** in solution and gel were compared. Two absorption bands at 347 and 434 nm of solution **NN-3** in DMF/H_2O (v/v, 5/1) were turned into 347, 370 and 453 nm for gel **NN-3**, which indicated the J-aggregate mode was existed in gel (Fig. S3a in Supporting information) [48]. Two absorption bands at 347 and 440 nm of gel **NN-3** formed in DMSO/H_2O (v/v, 10/1) did not have any shift (Fig. S3b in Supporting information). In Fig. S3c (Supporting information), the absorption band at 431 nm of solution **NN-4** was red-shifted to 437 nm in gel **NN-4** in DMF/H_2O (v/v, 5/1). UV-vis absorption band at 350 nm of solution **NN-4** was red-shifted to 365 nm for gel **NN-4** in DMSO/H_2O (v/v, 10/1) (Fig. S3d in Supporting information). The absorption band of gels **NN-4** from acetonitrile/H_2O (v/v, 10/1) and ethanol/H_2O (v/v, 10/1) was not shifted (Figs. S3e and f in Supporting information). These results showed that **NN-3** and **NN-4** had the different self-assembly modes in different solvents. Emission peaks at 433 and 536 nm of solution **NN-3** in DMF/H_2O (v/v, 5/1) were red-shifted to 450 and 559 nm in gel state, and indicating π-π stacking in gel (Fig. S4a in Supporting information). In addition, the emission intensity at 450 nm was further decreased in gel state due to the enhanced energy transfer. The similar fluorescence change from solution to gel state was observed in Figs. S4b-f (Supporting information). Comparing with our previous reported naphthalimide-based gel system [49], the small red-shift from solution to gel indicated that amino in naphthalimide went against π-π stacking between aromatic structures to some extent [50].

In FTIR spectra of xerogels **NN-3**, N-H stretching peaks of 3365, 3357 cm^{-1} and the stretching peak of C=O at 1647 and 1648 cm^{-1} indicated that hydrogen bonding played a significant role in the formation of gel (Fig. S5a in Supporting information). The similar N-H and C=O stretching peaks were observed in FTIR spectra of xerogels **NN-4** (Fig. S5b in Supporting information). As shown in Figs. S6a, b, e and f (Supporting information), XRD patterns of xerogels **NN-3** and **NN-4** from DMF/H_2O (v/v, 5/1) exhibited a series of diffraction peaks, which demonstrated that self-assembly of **NN-3** and **NN-4** was highly ordered. Rare diffraction peaks in that of xerogels **NN-3** and **NN-4** from other solvents indicated that self-assemblies of **NN-3** and **NN-4** in these gels were in the long range disorder (Figs. S6c, d and g-l in Supporting information). The diffraction peaks with *d*-space values of 0.40, 0.41, 0.39, 0.42, 0.38 and 0.38 nm should be π-π stacking between naphthalimide group [51].

$(COCl)_2$, DCP, DECP, DMMP, $POCl_3$, phosgene, $SOCl_2$, TsCl and CH_3COCl were selected to investigate the selectivity of **NN-3** and **NN-4** towards acyl chloride (Fig. 4). Upon addition of 1.0 equiv. of $(COCl)_2$ and phosgene, the emission peak at 476 nm of solution **NN-3** was blue-shifted to 426 and 437 nm with intensity enhancement, respectively (Fig. 4a). For other acyl chlorides, a weak fluc-

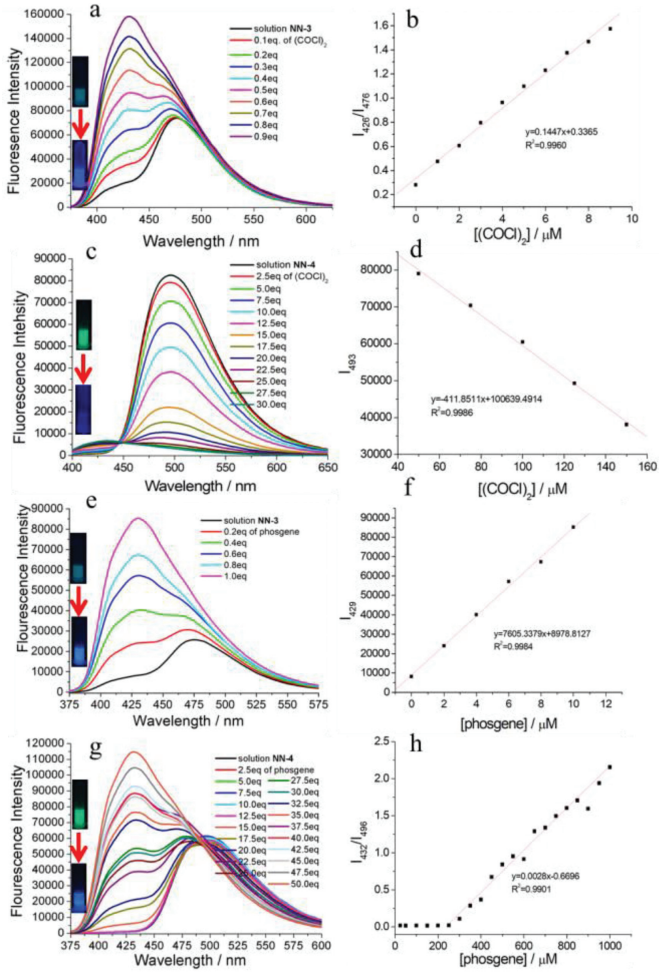

Fig. 5. (a, c, e, g) Fluorescence spectra of solutions **NN-3** and **NN-4** (10 μmol/L) under the titration of $(COCl)_2$ and phosgene. (b, d, f, h) Linear relationship of the fluorescence emission intensity at respective versus the concentration of phosgene and $(COCl)_2$; The inset figures were images of solutions **NN-3** and **NN-4** before and after titration of phosgene and $(COCl)_2$ under 365 nm light lamp, μM is μmol/L.

tuation was observed. For solution **NN-4**, 5.0 equiv. of $(COCl)_2$ and phosgene were added, fluorescence emission was also blue-shifted from 494 nm to 437 and 432 nm along with the emission intensity significant quenching and enhancing, respectively (Fig. 4b). Upon the addition of $(COCl)_2$ and phosgene to solutions **NN-3** and **NN-4**, absorption band in the visible region were obviously decreased (Figs. S7a and b in Supporting information). The photographs of solutions **NN-3** and **NN-4** well validated the fluorescence and absorption change (Fig. S7c in Supporting information).

In order to further study the detection performance of **NN-3** and **NN-4**, the titration experiments of solutions **NN-3** and **NN-4** by phosgene and $(COCl)_2$ were done by fluorescence and UV-vis absorption spectra. With the addition of $(COCl)_2$, the fluorescence emission at 476 nm of solution **NN-3** was weakly enhanced along with an appearance of new emission peak at 426 nm, which showed intramolecular ET was restrained (Fig. 5a). A good linear relationship between the ratio of emission intensity at 476 and 426 nm (F_{426}/F_{476}) was constructed with the LOD of 210 nmol/L on the base of LOD = $3\sigma/b$ (Fig. 5b) [52]. With the addition of $(COCl)_2$ to solution **NN-4**, fluorescence emission at 493 nm was gradually lessened (Fig. 5c). The linear equation was constructed in the range of 40-160 μmol/L with the LOD of 12.4 μmol/L (Fig. 5d). When solution **NN-3** was titrated by phosgene, the emission intensity at 476 nm was slightly fluctuated, and the new emission peak was

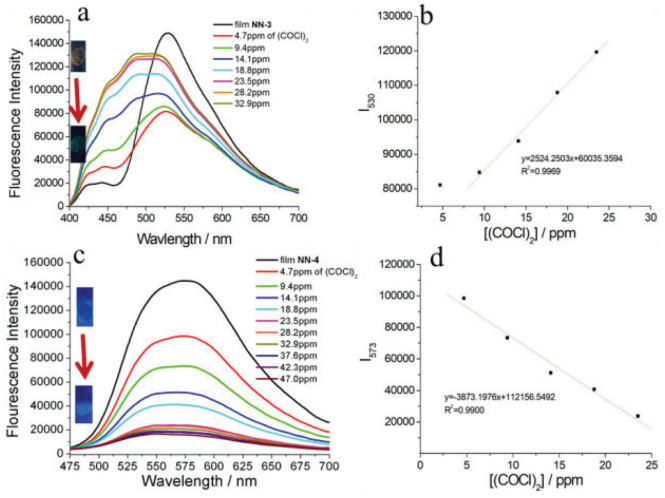

Fig. 6. (a, c) Fluorescence spectra of films **NN-3** and **NN-4** under the titration of $(COCl)_2$ gas. (b, d) The curved of the fluorescence emission intensity at 530 nm and 573 nm versus of films **NN-3** and **NN-4** with the concentration of $(COCl)_2$ respectively.

emerged at 429 nm with heightening by 3 times (Fig. 5e). A linear relationship was founded in scope of 0-10 μmol/L with the LOD of 90 nmol/L (Fig. 5f). In the presence of phosgene, the emission intensity at 431 nm of solution **NN-4** was gradually enhanced accompanying with no change about 495 nm (Fig. 5g). The liner relationship between the ratio of emission at 432 and 496 nm and the concentration of phosgene was generated with the LOD of 64 μmol/L (Fig. 5h). Emission light of solutions **NN-3** and **NN-4** was changed from green to blue (the inset images in Fig. 5). In the titration process, the isobestic points at 386, 401, 375 and 377 nm in UV-vis absorption spectra indicated that new compounds were produced (Fig. S8 in Supporting information). Fluorescence kinetics of solutions **NN-3** and **NN-4** towards $(COCl)_2$ and phosgene exhibited the different response times (Fig. S9 in Supporting information). With the addition of $(COCl)_2$ and phosgene, solution **NN-3** needed 50 s and 150 min for reaching to its destination and half of the maximum, respectively (Figs. S9a and b). For solution **NN-4**, it needed 3 min and 250 min to arrive at its half of the minimum and maximum, respectively (Figs. S9c and d). $(COCl)_2$ and phosgene could be differentiated by **NN-3** and **NN-4** *via* the response speed. In addition, the selectivity of **NN-3** and **NN-4** was investigated in THF (Fig. S10 in Supporting information). The experimental results showed that solution **NN-3** in THF responded to $SOCl_2$ and phosgene, but solution **NN-4** in THF did not obviously respond any kind of analytes. The different selectivity of **NN-3** and **NN-4** in CH_2Cl_2 and THF was possible due to the solvent effect on nucleophilic reaction.

In terms of three-dimensional network with large contacting area in gel systems, it endowed the convenience for analytes into the interior [53,54]. Solutions **NN-3** and **NN-4** in CH_2Cl_2 were coated onto quartz plate and prepared into film structure *via* the fast volatilization of CH_2Cl_2. Nanofibers structure and irregular nanospheres was observed in films **NN-3** and **NN-4**, respectively (Fig. S11 in Supporting information). The selectivities of films **NN-3** and **NN-4** towards different chlorides were firstly investigated one by one (Fig. S12 in Supporting information). As shown in Fig. S12, films **NN-3** and **NN-4** exhibited the selectivity only towards $(COCl)_2$. When film **NN-3** was contacted with $(COCl)_2$ gases with the concentration of 4.7 ppm, emission intensity at 530 nm was quenched by about 50% (Fig. 6a). With the concentration of $(COCl)_2$ gas increasing, a wide emission peak at 488 nm was appeared along with its intensity enhancement. LOD of film **NN-3** towards $(COCl)_2$ gases was calculated as 2.0 ppm (Fig. 6b). Emission of film **NN-3** was changed into blue light from yellow light (inset in Fig. 6a). Emission of film **NN-4** at 573 nm was weakened by about 86.7% in the titration process (Fig. 6c). The emission change of film **NN-4** was well proved by the inserted images in Fig. 6c. LOD of film **NN-4** towards $(COCl)_2$ gases was calculated as 8.34 ppm according to the linear equation (Fig. 6d). The fluorescence kinetics experiments of films **NN-3** and **NN-4** towards $(COCl)_2$ gas exhibited the response time of 1 min and 5 min, respectively (Fig. S13 in Supporting information). Unfortunately, films **NN-3** and **NN-4** did not work as sensor for phosgene.

To reveal the detection mechanism of **NN-3** and **NN-4** toward phosgene and $(COCl)_2$, ^1H NMR and HRMS experiments were done. After reacting with phosgene and $(COCl)_2$, the chemical shift of NH_2- in molecule **NN-3** was shifted from 5.92 ppm to 5.93 ppm and 5.85 ppm, respectively, then the integration of amine group was reduced from 1.71 to 1.0 and 0.75 (Fig. S14 in Supporting information). HRMS data of **NN-3** with 691.25 was turned into 713.25 and 741.25 in Fig. S16 (Supporting information). The reaction products from **NN-3** reaction with phosgene and $(COCl)_2$ were speculated in Figs. S14 and S16. The reaction of **NN-3** and phosgene and $(COCl)_2$ produced an amide group along with another chlorine atom changing into hydroxyl group. The similar reaction was also occurred on **NN-4**. After **NN-4** reacted with phosgene, the NMR peak at 7.33 ppm of NH_2– of molecule **NN-4** was greatly minished and the wide NMR peak at 10.43 should be assigned to the carboxy group (Fig. S15 in Supporting information). NMR peak of $–NH_2$ of molecule **NN-4** was significantly decreased, but the wide NMR peak belonged to the carboxy group was not appeared for the reaction of **NN-4** and $(COCl)_2$. HRMS change about the reaction process of **NN-4** with phosgene and $(COCl)_2$ was also observed in Fig. S17 (Supporting information), and the corresponding molecule structures of **NN-4** was provide in Figs. S15 and S17. The simplified precursor compounds **1**-**3** and the corresponding products from compounds **2**-**3** reaction with $(COCl)_2$ and phosgene were subjected to theoretical calculation for further understanding the emission change of **NN-3** and **NN-4** (Fig. S18 in Supporting information). The energy gaps between HOMO and LUMO of the simplified compounds **1**-**3** was 3.9 eV, 3.56 eV and 3.66 eV, respectively. After compound **2** reacted with $(COCl)_2$ and phosgene, the energy gaps of its corresponding product were 3.82 eV and 3.83 eV, which indicated UV-vis absorption of the product was blue-shifted to low wavelength, and further decreased the intramolecular energy transfer efficiency. The semblable theoretical calculation results were also occurred on compound **3** in Fig. S18. Theoretical calculation results explained the photophysical properties change in the detection process.

In conclusion, we designed and developed two gelators **NN-3** and **NN-4** based on naphthalimide derivatives with the gelation capability in some solvents. Difference about the position of the amino group in **NN-3** and **NN-4** could lead to their differences in gelation ability, photophysical properties, and self-assembly structures. Interestingly, **NN-3** and **NN-4** both exhibited high selectivity for $(COCl)_2$ and phosgene, and they could be distinguished by the response time. **NN-3** and **NN-4** exhibited the shorter response time towards $(COCl)_2$ than phosgene. While **NN-3** has a lower LODs towards $(COCl)_2$ and phosgene than these of **NN-4** due to the high reactivity of amino group at 3- position. $(COCl)_2$ and phosgene was detected in solution and gases states by **NN-3** and **NN-4**. LODs of solutions **NN-3** and **NN-4** towards $(COCl)_2$ and phosgene were 0.21 μmol/L, 90 nmol/L, 12.4 μmol/L and 64 μmol/L, respectively. LODs of films **NN-3** and **NN-4** towards $(COCl)_2$ by were 2.0 ppm and 8.34 ppm. Based on these data, we expect that probes **NN-4** and **NN-3** to be an effective tool for detecting $(COCl)_2$ and phosgene. Overall, this work may offer a facile, visual and sensitive method for rapid detection of $(COCl)_2$ and phosgene in solution and gas phase.

Declaration of competing interest

The authors declare that there are no conflicts of interest.

Acknowledgments

This work was financially supported by the National Natural Science Foundation of China (No. U1704164), the Basic Research Project of Henan Provincial Key Scientific Research Project (No. 22ZX002).

Supplementary materials

Supplementary material associated with this article can be found, in the online version, at doi:10.1016/j.cclet.2022.06.067.

References

[1] X. Jin, Y. Sang, Y. Shi, et al., ACS Nano 13 (2019) 2804–2811.
[2] K. Li, S. Chen, X. Zhu, et al., Mater. Chem. Front. 6 (2022) 593–599.
[3] X.Z. Li, C.B. Tian, Q.F. Sun, Chem. Rev. 122 (2022) 6374–6458.
[4] L. Ma, Q. Xu, S. Sun, et al., Angew. Chem. Int. Ed. 61 (2022) e202115748.
[5] Y. Li, J.G. Yu, L.L. Ma, et al., Sci. China Chem. 64 (2021) 701–718.
[6] Y.W. Zhang, S. Bai, Y.Y. Wang, et al., J. Am. Chem. Soc. 14 (2020) 13614–13621.
[7] D. Xia, P. Wang, X. Ji, et al., Chem. Rev. 120 (2020) 6070–6123.
[8] H. Xu, C. Zhou, C. Jian, et al., Chin. Chem. Lett. 31 (2020) 369–372.
[9] C. Li, S. Cao, J. Lutzki, et al., J. Am. Chem. Soc. 144 (2022) 3083–3090.
[10] X. Cheng, M. Li, H. Wang, et al., Chin. Chem. Lett. 31 (2020) 869–874.
[11] A. Chatterjee, A. Reja, S. Pal, et al., Chem. Soc. Rev. 51 (2022) 3047–3070.
[12] H. Zhang, Q. Li, Y. Yang, et al., J. Am. Chem. Soc. 143 (2021) 18635–18642.
[13] X. Cao, Y. Li, A. Gao, et al., J. Mater. Chem. C 7 (2019) 10589–10597.
[14] E. Olivieri, G. Quintard, J.V. Naubron, et al., J. Am. Chem. Soc. 143 (2021) 12650–12657.
[15] S.A. Holey, K.P.C. Sekhar, D.K. Swain, et al., ACS Biomater. Sci. Eng. 8 (2022) 1103–1114.
[16] F. Diehl, S. Hageneder, S. Fossati, et al., Chem. Soc. Rev. 51 (2022) 3926 -3663.
[17] Y. Zhao, S. Song, X. Ren, et al., Chem. Rev. 122 (2022) 5604–5640.
[18] B.O. Okesola, D.K. Smith, Chem. Soc. Rev. 45 (2016) 4226–4251.
[19] C. Wang, J. Zhang, ACS Appl. Bio Mater. 5 (2022) 1934–1953.
[20] S. Shahi, H. Roghani-Mamaqani, R. Hoogenboom, et al., Chem. Mater. 34 (2022) 468–498.
[21] Y. Gao, J. Zhao, Z. Huang, et al., Angew. Chem. Int. Ed. 61 (2022) e202201793.
[22] N. Nitta, M. Takatsuka, S.I. Kihara, et al., Angew. Chem. Int. Ed. 59 (2020) 16690–16697.
[23] S. Wang, L. Zheng, W. Chen, et al., CCS Chem. 2 (2020) 2473–2484.
[24] Y. Zhang, L. Wang, J. Wang, et al., Chin. Chem. Lett. 32 (2021) 1902–1906.
[25] X. Cao, A. Gao, J.T Hou, et al., Coord. Chem. Rev. 434 (2021) 213792.
[26] M. Hu, F.Y. Ye, C. Du, et al., Angew. Chem. Int. Ed. 61 (2022) e202115216.
[27] Y. Xiao, Q. Wang, X. Feng, et al., J. Mater. Chem. A 9 (2021) 17451–17458.
[28] P. Liao, Y. Hu, Z. Liang, et al., J. Mater. Chem. A 6 (2018) 3195–3201.
[29] T.L. Mako, J.M. Racicot, M. Levine, Chem. Rev. 119 (2019) 322–477.
[30] W.Q. Zhang, K. Cheng, X. Yang, et al., Org. Chem. Front. 4 (2017) 1719–1725.
[31] A.P. Vargas, F. Gamez, J. Roales, et al., ACS Sens. 3 (2018) 1627–1631.
[32] W. Li, M. Rosenbruch, J. Pauluhn, Exp. Toxicol. Pathol. 67 (2015) 109–116.
[33] C. Wu, G. Li, Q.B. Han, et al., Dalton Trans. 46 (2017) 17074–17079.
[34] L. Zeng, T. Chen, B. Zhu, et al., Chem. Sci. 13 (2022) 4523–4532.
[35] P. Sutar, T.K. Maji, Chem. Commun. 52 (2016) 8055–8074.
[36] M.L. Kuitunen, J.C. Altamirano, P. Siegenthaler, et al., Anal. Methods 12 (2020) 2527–2535.
[37] J. Beheshtian, A.A. Peyghan, Z. Bagheri, Sens. Actuator. B: Chem. 171–172 (2012) 846–852.
[38] P.V. Ravi, D.T. Thangadurai, D. Nataraj, et al., ACS Appl. Mater. Interf. 11 (2019) 19339–19349.
[39] B. Zhu, R. Sheng, T. Chen, et al., Coord. Chem. Rev. 463 (2022) 214527.
[40] N. Thirumalaivasan, S.P. Wu, ACS Appl. Biol. Mater. 3 (2020) 6439–6446.
[41] S.L. Wang, L. Zhong, Q.H. Song, Chem. Eur. J. 24 (2018) 5652–5658.
[42] T. Chen, L. Jiang, J.T. Hou, et al., J. Mater. Chem. A 8 (2020) 24695–24702.
[43] X.J. Wang, W.Q. Zhang, K. Cheng, et al., Org. Chem. Front. 4 (2017) 1719–1725.
[44] X. Cao, Q. Han, Q. Wang, et al., Colloid Surf. A 629 (2021) 127480.
[45] Q. Han, Q. Wang, H. Wu, et al., ChemistrySelect 7 (2022) e202200298.
[46] X. Cao, N. Zhao, A. Gao, et al., Langmuir 34 (2018) 7404–7415.
[47] X. Shen, W. Xu, J. Ouyang, et al., Chin. Chem. Lett. 33 (2022) 4505–4516.
[48] P. Bairi, B. Roy, P. Routh, et al., Soft Matter 8 (2012) 7436–7445.
[49] X. Cao, L. Meng, Z. Li, et al., Langmuir 30 (2014) 11753–11760.
[50] X. Cao, Y. Li, A. Gao, et al., J. Mater. Chem. C 7 (2019) 10589–10597.
[51] W. Miao, L. Zhang, X. Wang, et al., Langmuir 29 (2013) 5435–5442.
[52] J.T. Hou, B. Wang, Y. Zou, et al., ACS Sens. 5 (2020) 1949–1958.
[53] X. Chen, T. Zhang, Y. Han, et al., J. Mater. Chem. C 9 (2021) 9932–9940.
[54] P. Xue, J. Ding, Y. Shen, et al., J. Mater. Chem. C 5 (2017) 11532–11541.